Modeling Induction Machines for EMC-Analysis

Stefan-Peter Weber, Eckart Hoene, Stephan Guttowski, Werner John, Herbert Reichl
Fraunhofer Institute for Reliability and Microintegration, Berlin, Germany
Email: stefan-peter.weber@izm.fraunhofer.de

***Abstract*— EMC-analysis of power electronic systems is strongly supported by network simulations. Simulations at the system level provide not only the prediction of EMI but also deep insight into the EMC relevant effects. To model the system properly, it is necessary to model source and target of EMI and also all parts of the coupling paths. EMI-filters can be designed efficiently using network based modeling approaches.**
In this paper a model for induction machines' EMC behaviour simulation is parameterized in the frequency range from some kHz up to 100 MHz. The high-frequency characteristics of induction machines with power ratings from 370 W up to 45 kW are compared and a model library is set up for both, frequency and time domain.

I. Introduction

Figure 1 shows a common three-phase drive system with an inverter-fed induction machine. Hoene [1] and Guttowski [2] present basic methods for the EMC-design of power converters at the system level. Simulations at the system level provide not only the prediction of EMI but also deep insight into the EMC relevant effects. To model the system properly, it is necessary to model source and target of EMI and also all parts of the coupling paths. For the analysis of conducted EMI, the input impedances, the output impedances and the transfer behaviour of all parts must be known.
A number of models and its application in the context of power drive systems have been presented in the literature by Murai, Zhong and Grandi and others [1]–[8]. The modeling approaches are similar to that used in this paper with different focuses in the frequency range and accuracy.
In this paper a model for simulating induction machines' EMC behaviour is parameterized in the frequency range from some kHz up to 100 MHz. The high-frequency characteristics of induction machines with power ratings from 370 W up to 45 kW are compared and a model library is set up for both, frequency and time domain. EMI-filters can then be designed efficiently using network based modeling approaches.

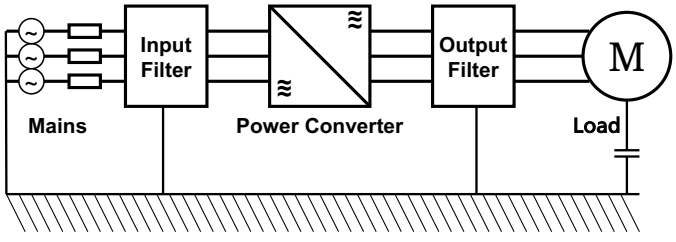

Fig. 1. EMC analysis of electric drive system

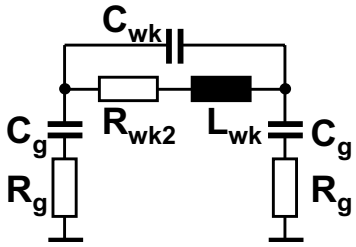

Fig. 2. Phase-belt winding model proposed by Zhong et al. in [4]

II. A High Frequency Model for Induction Machines

Murai et al. [3] investigated the calculation of average leakage current by adding a capacitance between the windings and the grounded stator core. An equivalent circuit for simulating common-mode and differential-mode behaviour, covering the EMI frequency range, is proposed by Zhong et al. in [4].
Since the distributed parameters of induction machine windings must be considered, Zhong et al. [4] propose grouping the coils of a phase-belt into basic elements such as shown in Figure 2.
The phase-winding model consists of a number of phase-belt windings connected in series. Thus, the effects of both, mutual magnetic coupling and the interturn capacitive coupling among the coils in a phase winding are modeled. Zhong et al. [4] modeled an induction machine with a single pair of poles and used four phase-belt windings connected in series. In the literature [5], [7], [8] distributed parameters are often avoided

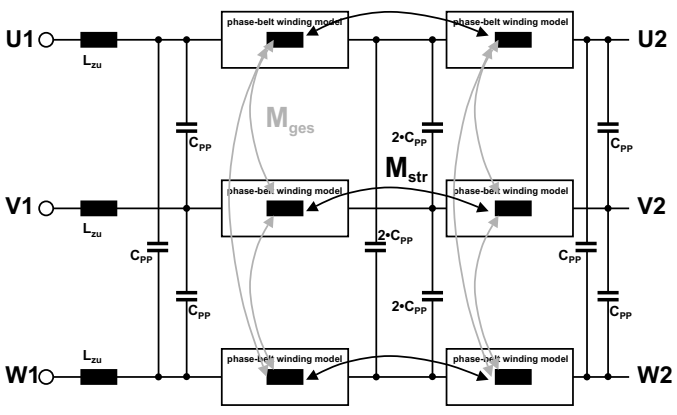

Fig. 3. Modeling induction machines with two basic elements per phase connected in series: inductances L_{wk} are mutually coupled by M_{ges} (omitting twelve coupling arrows for the benefit of a clear figure), windings of the same phase are additionaly coupled by M_{str}

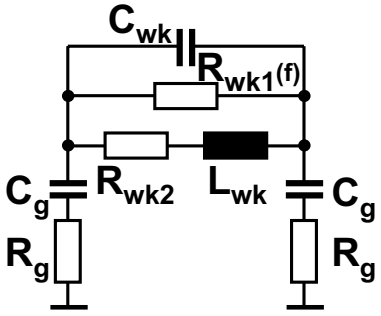

Fig. 4. Modeling one phase-belt winding

because identifying model parameters becomes more and more difficult.

Grandi et al. [6] use a series connection of two phase-belt windings and for the modeling approach in this paper a series connection of two π-shaped phase-belt windings will also be shown to be accurate.

All three phases are connected by inter-phase-capacitances. Very small inductances L_{zu} model the behaviour at frequencies higher than 10 MHz. Figure 3 shows the connections and coupling between the basic elements of the equivalent circuit for induction machines used in this paper.

Grandi et al. [6] added a resistance in parallel to the windings inductance. The resistance R_{wk1} (See Fig.4) makes it easier to take into account the AC iron loss, which increases linearly with frequency.

The use of frequency depending parameters is typically avoided in order to obtain equivalent circuits for both time and frequency domain simulations. As this paper focuses on RFI (Radio Frequency Interference) and considerations in the frequency domain, frequency dependent parameters are used to obtain models with high accuracy in the frequency range from some kHz up to 100 MHz. Whenever frequency dependent parameters are used in this paper, fixed values for time-domain calculations are also determined.

III. Parameter Identification

There are two measurements conducted with the induction machines in star connection.

Measuring the impedance between one phase and the two other phases using the setup shown in Figure 5 provides the differential-mode characteristics of the induction machine under test.

Measuring three shortened phases against ground using the setup shown in Figure 7 provides the common-mode characteristics.

The rotor is stationary. In Hoene [1] the influence of saturation is proved to be smaller than 2% of the impedance's absolute value with a 5.5kW induction machine. With frequencies higher than 80 kHz, the influence of the saturation disappears completely. Therefore a small-signal measurement is sufficient.

A. Differential Mode Characteristics

The parameter L_{sy}, the differential-mode inductance, is received directly from the differential-mode characteristics

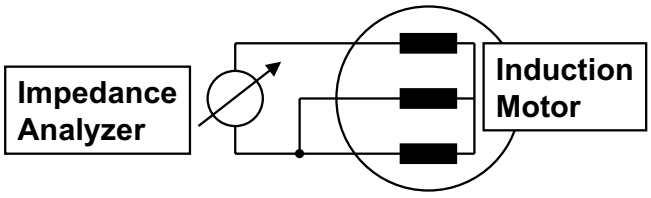

Fig. 5. Measurement setup for differential mode behaviour

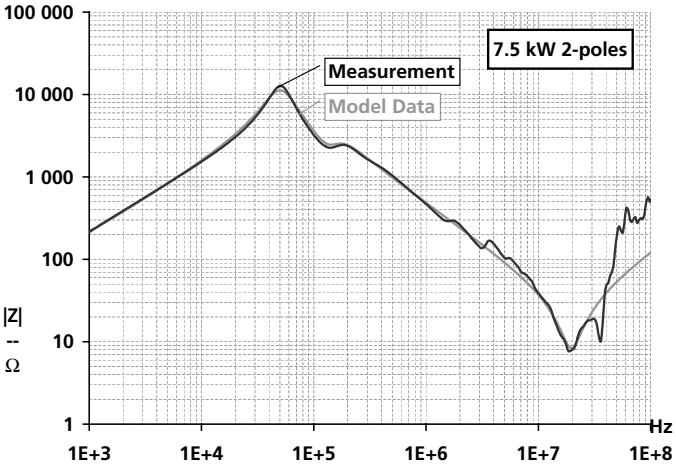

Fig. 6. Measurement and model data of a 7.5 kW induction machine's differential-mode impedance

measurement. L_{sy} is used to calculate M_{ges} and M_{str}(Section III-C). L_{wk}, M_{ges} and M_{str} model both differential-mode and common-mode behaviour. Furthermore, values for C_{pp}, L_{zu} and R_g are obtained from this measurement.

Figure 6 shows measurement and model data of the impedance of induction machine terminal U1 against the two other terminals V1 and W1. Until the first resonance at 51 kHz, the inductive impedance of this 7.5 kW machine is clearly documented. Impedance values from 1 kHz up to 50 kHz correspond to inductance values decreasing from 52 mH down to 24 mH by simply calculating $L = \frac{Z}{\omega}$. With rising frequency the reluctance seen by the differential-mode current increases due to diffusion. For time-domain simulations, 26 mH is a good value. For very accurate frequency-domain calculations $L_{sy} = (19.9 + \frac{0.4577}{\sqrt{f}})$ mH in case of this 7.5 kW machine.

For frequencies higher than 52 kHz the impedance is determined by capacitive coupling among the phases. In this case, a value of 1 pF is determined for C_{pp}. For frequencies higher than 1 MHz, minor structural resonances occur that are not seperately modeled. The resonance at 20 MHz provides $R_g = 8\Omega$. Above that resonance the impedance rises again with more than 20 dB per decade. L_{zu}=180 nH approximates this behaviour.

B. Common Mode Characteristics

The common-mode impedance is denoted by the transition from a higher capacitance to a lower one. The higher one is C_{gges} and is received directly from the common-mode

TABLE I

PARAMETERS MODELING HIGH-FREQUENCY BEHAVIOUR OF INDUCTION MACHINES

	370 W	750 W	1.5 kW	2.2 kW	4 kW	7.5 kW	7.6 kW	15 kW	45 kW
	Differential-Mode Characteristics								
L_{sy} in mH	200	100	30	100	16	26	12	13	4
C_{pp} in pF	3	0.2	0.5	0.5	1	1	70	220	100
L_{zu} in nH	60	200	300	250	110	180			750
R_g in Ω	29	28	20	14	10	8	8	8	8
	Common-Mode Characteristics								
C_{gges} in nF	1.1	1.7	1.9	3.4	3.1	4.9	3.3	3.4	9.5
f_{min} in kHz	65	70	100	46	110	75	230	220	70
L_{asy} in mH	5	3	1	4	0.7	0.9	0.1	0.2	0.5
C_{wk} in pF	50	85	12	1	10	90	250	850	450
	More Parameters								
L_{wk} in mH	32.0	16.5	8.0	25.0	3.7	4.4	1.6	2.8	6.0
k_{ges}	-0.2250	-0.1985	-0.0813	-0.1166	-0.1034	-0.1710	-0.3482	-0.2168	0.0310
k_{str}	0.0274	0.0136	0.0013	0.0054	0.0013	0.0035	0.0018	0.0009	-0.0045
R_{wk1} in kΩ	10.6	11.0	15.0	5.4	4.6	3.8	2.2	2.2	1.2

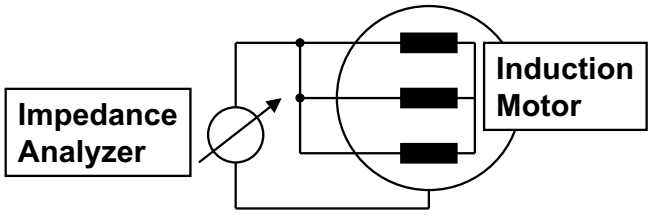

Fig. 7. Measurement setup for common mode behaviour

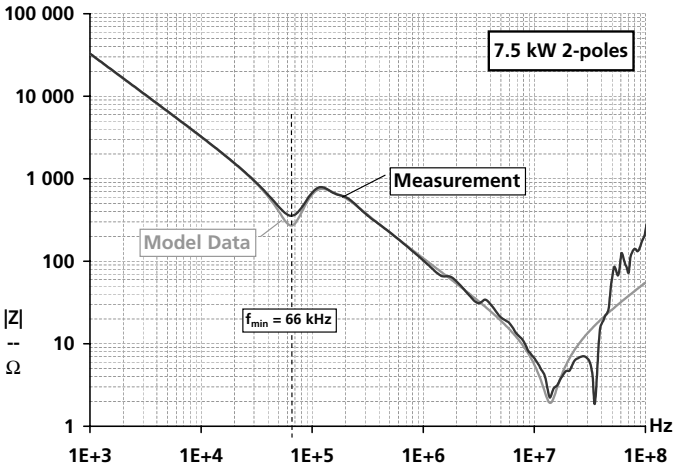

Fig. 8. Measurement and model data of a 7.5 kW induction machine's common-mode impedance

characteristics measurement at low frequencies. At the first resonance frequency L_{asy} shows up. The lower capacitance depends mainly on C_{wk}. L_{asy} is used to calculate M_{ges} and M_{str}(Section III-C).

Figure 8 shows measurement and model data of the impedance of the three shortened induction machine terminals UVW against the grounded stator iron. Impedance values at low frequencies provide C_{gges}=4.9 nF by simply calculating $C = \frac{1}{\omega Z}$. C_g is then the twelvth part of C_{gges}. The common-mode inductance L_{asy} is determined from the resonance frequency at 66 kHz:

$$L_{asy} = (\omega^2 C_{gges})^{-1} = 1.2mH \tag{1}$$

The capacitor C_{wk} is found to be 90 pF for correct impedance values up to some MHz. With frequencies higher than 1 MHz minor structural resonances occur that are not seperately modeled. The resonance at 14 MHz confirms $R_g = 8\Omega$, as determined above. The approximation of the behaviour above that resonance with L_{zu}=180 nH is well determined for the common-mode impedance aswell.

C. More Parameters to Be Defined

L_{wk} is given a value of some mH first, M_{ges} and M_{str} are then calculated according to Hoene [1]:

$$M_{ges} = -\frac{-27\ L_{asy} + 2\ L_{sy}}{36} \tag{2}$$

$$M_{str} = -\frac{36\ L_{wk} - 27\ L_{asy} - 10\ L_{sy}}{36} \tag{3}$$

Thus, the inductance network provides L_{sy} and L_{asy} independant of L_{wk}. R_{wk2} is small: 200 mΩ. The resonances between 30 kHz and 3 MHz are damped by R_{wk1}. R_{wk1} is initially given a high value such as 100 kΩ to illustrate the undamped case and the undamped resonances can clearly be seen using network simulation software. L_{wk} is determined to be 4.4 mH for the correct resonance frequencies in that range for the 7.5 kW induction machine. R_{wk1} changes linearly with the frequency. For time-domain simulations, 3.8 kΩ is a good value.

IV. COMPARISON OF INDUCTION MACHINES

Nine types of induction machines with power ratings from 370 W up to 45 kW have been modeled in the described manner. The models are based on measurements of two

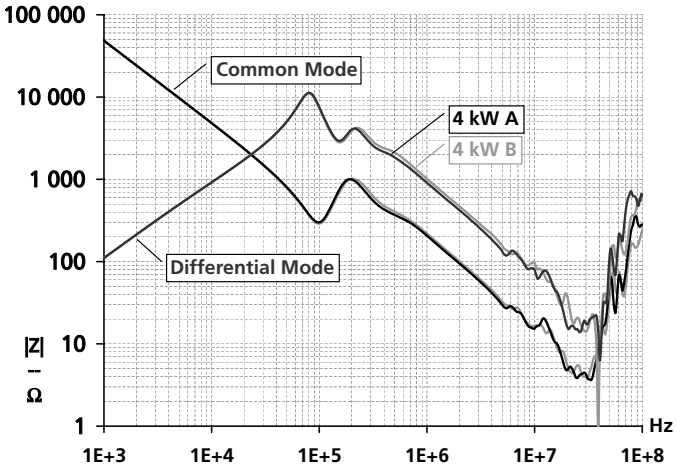

Fig. 9. Different impedance of two identic induction machines with 4.4 kW

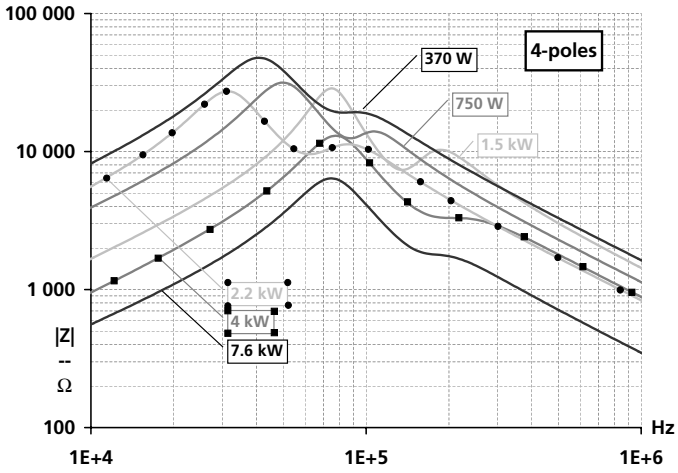

Fig. 10. Differential-mode impedance of induction machines with four poles

exemplars of each type. Now the question is to be dicussed: How representative are these nine machines in order to build up a library for systematic design of EMC measures. Can we expect other machines to have HF-impedances in between the modeled ones? Two answers on that questions can be given:
1) Exemplars of the same machine type do have similar HF-impedances.
2) Each machine type has its own characteristics and it is difficult to identify trends of the parameters according to the size and the power rating of the machines. For some parameters trends are clearly seen for others not. Thus, it is worthwhile modeling every single machine for the design of EMC measures. Nevertheless simulating with realistic models of the proposed power ratings helps obtaining statements on EMC design if there is no time to model every single machine.

A. Exemplars Do Have Similar HF-Impedances

From the nine machine types two exemplars' impedances are measured. Figure 9 shows a comparison of the two exemplars A and B of the 4.4 kW machine. Exemplars of the same machine type do have identical parameters at low frequencies. At higher frequencies differences occur that are in the range of the modeling accuracy. The results for the other eight machine types are equivalent.

B. Each Type of Machines Has Its Own Characteristics

As the power rating increases, and thus the size of the induction machine, one expects rising capacitances due to larger areas of conducting materials facing each other separated. Inductances depend strongly on the design of the machines in terms of number of windings and coil configurations.
Figure 10 shows the differential-mode impedance of the four-pole induction machines with power ratings from 370 W to 7.6 kW. With the exception of the 2.2 kW machine, the inductances L_{sy} seen at low frequencies decrease with size.
For the inter-phase capacitances C_{pp} seen at higher frequencies no clear trend can be stated. The capacitances depend on other parameters than just the size of the induction machine such as different configurations of the coils' winding head.

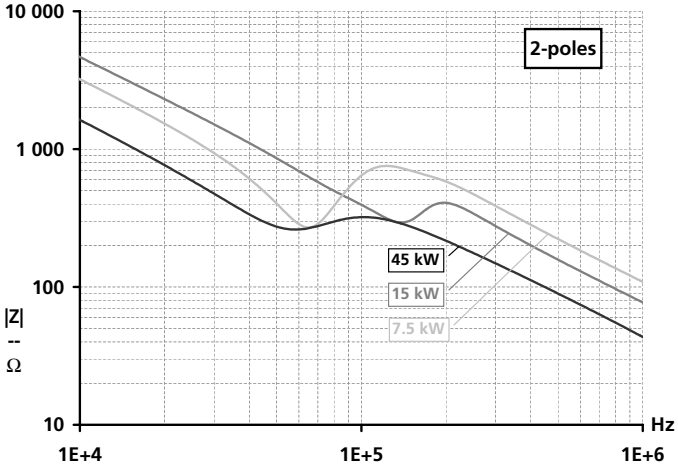

Fig. 11. Common-mode impedance of induction machines with two poles

Figure 11 shows the common-mode impedance of the two-pole induction machines with power ratings from 7.5 kW to 45 kW.
At low frequencies the capacitance to ground C_{gges} is documented in this diagram. The 45 kW induction machine has the highest capacitance to ground as expected, but the 7.5 kW machine's capacitance is much higher than the 15 kW's. At higher frequencies the capacitances match our expectations.
Table I lists the determined parameters. Each induction machine has its own characteristics and it is difficult to identify trends of the parameters according to the size and the power rating of the induction machines. Considering the wide range of configurations of induction machines' windings and technology parameters, the difficulties in identifying trends are evident.
The parameters that corelate best with the size and the power rating of the induction machines are the resistances R_g and R_{wk1}. Representing the loss in the path of common-mode currents and loss due to induced currents in the stator core, the resistances R_g and R_{wk1} decrease noticeable with the size of the induction machine. For some parameters trends are clearly seen for others not. Thus, it is worthwhile modeling every

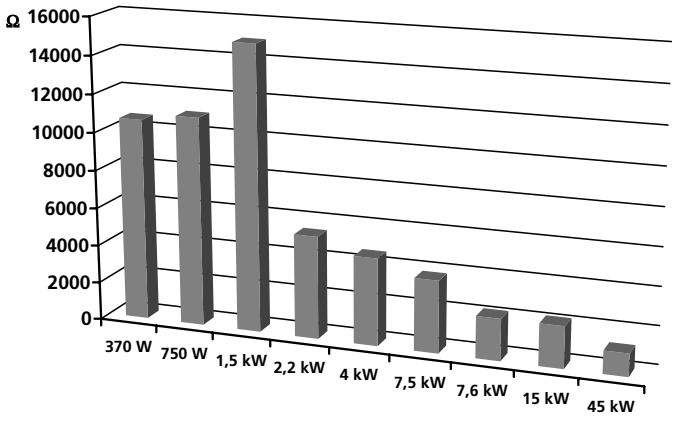

Fig. 12. R_{wk1} representing loss due to induced currents in the stator core

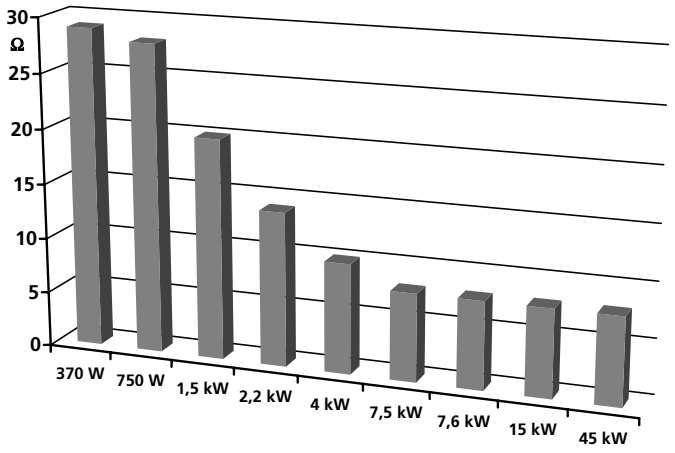

Fig. 13. R_g representing loss due to common-Mode currents

single machine for the design of EMC measures. Nevertheless simulating with realistic models of the proposed power ratings helps obtaining statements on EMC design if there is no time to model every single machine.

V. Conclusion

For the analysis of conducted EMI, the input impedances, the output impedances and the transfer behaviour of all parts of common mode and differential mode coupling paths between source and target of EMI must be known.

In this paper a model for simulating EMC behaviour of induction machines is parameterized in the frequency range from some kHz up to 100 MHz. EMC behaviour of induction machines with power ratings from 370 W up to 45 kW is compared and a model library is set up for both, frequency and time domain. Trends of model parameters over the size and power rating of the induction machines are identified where possible.

Although it is much better to have a model for every single machine considered in an EMC design process, a model library was built from the available data. Simulating realistic models over the proposed power ratings helps to obtain information on EMC design when there is no time to model every single machine.

References

[1] Eckart Hoene, *Methoden zur Vorhersage, Charakterisierung und Filterung elektromagnetischer Stoerungen von spannungsgespeisten Pulswechselrichtern*, Dissertation TU Berlin, VDI Verlag, Duesseldorf, 2001

[2] Stephan Guttowski, *Untersuchungen zur elektromagnetischen Vertraeglichkeit spannungsgespeister Pulswechselrichter*, Dissertation TU Berlin, Verlag Dr.Koester, Berlin, 1998

[3] Y.Murai, T.Kubota, Y.Kawase, *Leakage Current Reduction for a High-Frequency Carrier Inverter Feeding an Induction Motor*, IEEE Transactions on Industry Applications, vol.28, no.4, 1992

[4] E.Zhong, T.A.Lipo, *Improvements in EMC Performance of Inverter-Fed Motor Drives*, IEEE Transactions on Industry Applications, 1995

[5] A.Consoli, G.Oriti, A.Testa, A.L.Julian, *Induction Motor Modeling for Common Mode and Differential Mode Emission Evaluation*, IEEE Industry Applications Conference, 1996

[6] G.Grandi, D.Casadei, A.Massarini, *High Frequency Lumped Parameter Model for AC Motor Windings* Proc. EPE, vol.2, Trondheim, Norway, 1997

[7] A.Boglietti, E.Carpaneto, *Induction Motor High Frequency Model*, IEEE Industry Applications Conference, 1999

[8] A.Moreira, T.Lipo, G.Venkataramanan, S.Bernet *High-Frequency Modeling for Cable and Induction Motor Overvoltage Studies in Long Cable Drives*, IEEE Transactions on Industry Applications, Vol.38, No.5, 2002